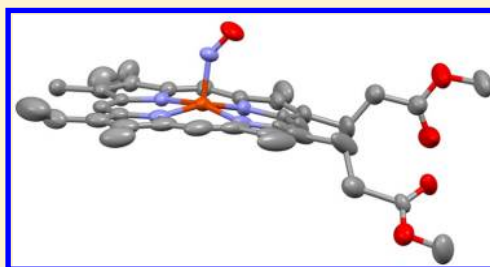


## Iron Nitrosyl “Natural” Porphyrinates: Does the Porphyrin Matter?

Graeme R. A. Wyllie,<sup>‡,¶</sup> Nathan J. Silvernail,<sup>‡,¶</sup> Allen G. Oliver,<sup>‡</sup> Charles E. Schulz,<sup>§</sup> and W. Robert Scheidt<sup>\*,‡</sup><sup>‡</sup>Department of Chemistry and Biochemistry, University of Notre Dame, Notre Dame, Indiana 46556, United States<sup>§</sup>Department of Physics, Knox College, Galesburg, Illinois 61401, United States

## S Supporting Information

**ABSTRACT:** The synthesis and spectroscopic characterization of three five-coordinate nitrosyliron(II) complexes,  $[\text{Fe}(\text{Porph})(\text{NO})]$ , are reported. These three nitrosyl derivatives, where Porph represents protoporphyrin IX dimethyl ester, mesoporphyrin IX dimethyl ester, or deuteroporphyrin IX dimethyl ester, display notable differences in their properties relative to the symmetrical synthetic porphyrins such as OEP and TPP. The N–O stretching frequencies are in the range of  $1651\text{--}1660\text{ cm}^{-1}$ , frequencies that are lower than those of synthetic porphyrin derivatives. Mössbauer spectra obtained in both zero and applied magnetic field show that the quadrupole splitting values are slightly larger than those of known synthetic porphyrins. The electronic structures of these naturally occurring porphyrin derivatives are thus seen to be consistently different from those of the synthetic derivatives, the presumed consequence of the asymmetric peripheral substituent pattern. The molecular structure of  $[\text{Fe}(\text{PPIX-DME})(\text{NO})]$  has been determined by X-ray crystallography. Although disorder of the axial nitrosyl ligand limits the structural quality, this derivative appears to show the same subtle structural features as previously characterized five-coordinate nitrosyls.



## ■ INTRODUCTION

It has been just over two decades since the role of nitric oxide (NO) as an essential biological signaling agent was recognized and which led to its selection as *Science's* molecule of the year in 1992.<sup>1</sup> NO is now recognized for its importance in blood pressure regulation, as a neurotransmitter, as well as a (toxic) defense mechanism in neutrophils and macrophages.<sup>2–13</sup>

Iron(II) porphyrinates are one of the critical biological targets of NO, and extensive work has characterized the iron nitrosyl unit in a range of synthetic porphyrin model complexes  $[\text{Fe}(\text{Porph})(\text{NO})]$ .<sup>14–16</sup> However, information from early crystallographic studies was limited due to severe problems with disorder of the NO ligand.<sup>17–19</sup> It was only with the report of two ordered crystalline polymorphs of the five-coordinate (nitrosyl)iron(II) porphyrinate derivative  $[\text{Fe}(\text{OEP})(\text{NO})]$ <sup>20</sup> that hitherto unobserved structural trends became apparent, trends that have been since observed in a number of other iron(II) nitrosyl porphyrinates.<sup>16,21</sup> In these structures, the  $\text{FeN}_5$  coordination group shows substantial deviation from an ideal symmetric coordination, with a significant off-axis tilt of the  $\text{Fe–N}(\text{NO})$  bond vector and an apparently correlated asymmetry in the equatorial  $\text{Fe–N}_p$  bond distances. This equatorial asymmetry pattern is displayed wherein the two  $\text{Fe–N}_p$  bonds closest to the tilted  $\text{Fe–N}(\text{NO})$  axial vector are effectively identical but significantly shorter than the other two  $\text{Fe–N}_p$  bonds, which are also effectively equal to each other. The tilting/asymmetry pattern has also been observed in a cobalt system, although the deviations from ideal axial symmetry are smaller.<sup>22</sup>

Further studies focused on preparing a series of additional five-coordinate (nitrosyl)iron(II) porphyrinate derivatives that vary in the nature and the position of the  $\beta$ -pyrrolic- and meso-substituents. Characterization of derivatives of a  $\beta$ -oxochlorin and the asymmetrically substituted 2,3,12,13-tetrabromo-5,10,15,20-tetraphenylporphyrin revealed the same tilt/asymmetry pattern observed in the  $[\text{Fe}(\text{OEP})(\text{NO})]$  derivatives.<sup>21</sup> To date there is only one structure reported for a naturally occurring porphyrin derivative, that of  $[\text{Fe}(\text{DPIX-DME})(\text{NO})]$ .<sup>23</sup> This structure displayed the same off-axis tilting as previously observed in the synthetic porphyrins, with the tilt direction lying in the direction of the two pyrrole rings bearing the propionate groups.

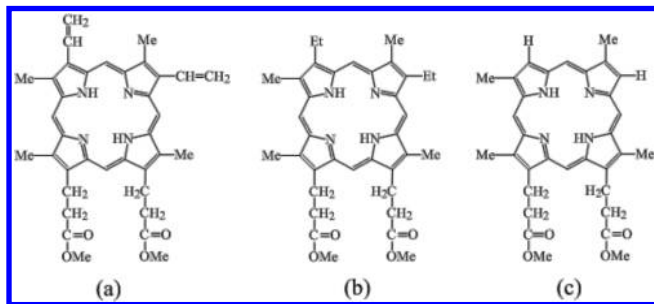
However, despite these similarities, physical characterization of these naturally occurring porphyrin derivatives showed some significant differences from the synthetic porphyrins. Initial investigation of the vibrational spectra of nitrosyl iron derivatives utilizing nuclear resonance vibrational spectroscopy (all taken as powder spectra) showed that the in-plane components of the iron vibrational spectra were surprisingly sensitive to the nature of the peripheral groups. Even changing only two substituents in the trio of naturally occurring porphyrins (protoporphyrin IX, deuteroporphyrin IX, and mesoporphyrin IX, shown in Scheme 1) had observable effects on the in-plane vibrational spectra.<sup>24</sup>

To further investigate the differences between the naturally occurring and synthetic porphyrins, we report the synthesis of

Received: January 14, 2014

Published: March 12, 2014

**Scheme 1. Diagrams Giving the Structure for (a) Protoporphyrin IX Dimethyl Ester, (b) Mesoporphyrin IX Dimethyl Ester, (c) Deuteroporphyrin IX Dimethyl Ester**



[Fe(Porph)(NO)] derivatives based on the trio of naturally occurring porphyrins. These derivatives have been characterized by UV–vis, IR, and EPR spectroscopy. In addition, the three derivatives have been characterized by Mössbauer spectroscopy in zero and applied magnetic field. After significant effort, single crystals of [Fe(PPIX-DME)(NO)] have been obtained, and the X-ray structure has been determined. Unfortunately, the axial NO ligand displays some disorder.

## EXPERIMENTAL SECTION

**General Information.** All reactions and manipulations of the iron(II) porphyrin derivatives were carried out under argon using a double-manifold vacuum line, Schlenkware, and cannula techniques. Dichloromethane, chloroform, methanol, and hexanes were distilled under argon over CaH<sub>2</sub>, magnesium turnings, and sodium/benzophenone, respectively. The free bases, protoporphyrin IX dimethyl ester, deuteroporphyrin IX dimethyl ester, and mesoporphyrin IX dimethyl ester, were purchased from Frontier Scientific. Nitric oxide (Mittler Specialty Gases) was purified by fractional distillation through a trap containing 4A molecular sieves bathed in a dry ice/ethanol slurry.<sup>25</sup>

**Synthetic Information.** Iron(II) chloride was purchased from Acros. Insertion of iron into H<sub>2</sub>(PPIX-DME), H<sub>2</sub>(DPIX-DME), or H<sub>2</sub>(MPIX-DME) was accomplished by the reaction of the free base and iron(II) chloride in DMF.<sup>26</sup> The desired five-coordinate [Fe(Porph)(NO)] derivative was obtained by reductive nitrosylation. Chloroporphyrinatoiron(III) compounds were reductively nitrosylated<sup>17</sup> under argon, and all solvents used were degassed by sparging with argon for 5 min. Liquid–liquid diffusion crystallization was done with chloroform solutions and with methanol as the counter solvent in 40 cm × 7 mm glass tubes, sealed with rubber septa. Crystals were typically harvested after about 10 days and washed with methanol. Crystals of [Fe(PPIX-DME)(NO)] and [Fe(DPIX-DME)(NO)] were thus obtained. The obtained crystals of [Fe(DPIX-DME)(NO)] are a new polymorphic form. Unfortunately, the crystal structure determination of the new DPIX-DME derivative was only partly successful; the successful PPIX-DME determination is reported herein.

**Spectral Data.** All three complexes were characterized by UV–vis, IR, EPR, and Mössbauer spectroscopies. UV–vis spectra were recorded in chloroform solution on a Perkin-Elmer Lambda 19 spectrometer. IR spectra were recorded on a Perkin-Elmer model 883 as KBr pellets. EPR spectra were recorded at 77 K with an X-band Varian E-12 spectrometer. Frozen solution spectra were obtained in dichloromethane glasses. Mössbauer measurements were performed on a constant acceleration spectrometer at 4.2 K in zero field and at 4.2 K in 4 and 9 T fields using a superconducting magnet system (Knox College).

**X-ray Structure Determination.** Single crystal experiments on [Fe(PPIX-DME)(NO)] were carried out on a Bruker Apex II system with graphite-monochromated Mo K $\alpha$  radiation ( $\lambda = 0.71073$  Å). A dark-red crystal with the dimensions 0.44 × 0.35 × 0.09 mm<sup>3</sup> was used

for the structure determination. The crystalline sample was placed in inert oil, mounted on a glass pin, and transferred to the cold gas stream of the diffractometer. Crystal data were collected at 100 K. The structure was solved by direct methods and refined against  $F^2$  using SHELXL;<sup>27</sup> subsequent difference Fourier syntheses led to the location of all remaining non-hydrogen atoms. For the structure refinement, all data were used, including negative intensities.

The asymmetric unit contains one independent porphyrin molecule and one not quite fully occupied chloroform solvate. Unfortunately, the structure is somewhat marred by disorder; most significantly, the oxygen atom of the nitrosyl ligand is found in two distinct locations with occupancies of 0.66(2) and 0.34(2). The carbonyl group of one of the propionate ester side arms is also disordered with two positions for the C=O moiety. The chloroform solvate molecule was also found to be disordered with two different orientations of the solvate, centered on the same carbon atom position. All non-hydrogen atoms were refined anisotropically. Hydrogen atoms were idealized with the standard SHELXL idealization methods. Brief crystallographic information is given in Table 1. Complete crystallographic details, atomic coordinates, anisotropic thermal parameters, and hydrogen atom coordinates are given in the Supporting Information.

**Table 1. Brief Crystallographic Data and Data Collection Parameters**

formula	C <sub>36.91</sub> H <sub>36.88</sub> Cl <sub>2.68</sub> FeN <sub>5</sub> O <sub>5</sub>
FW, amu	781.14
<i>a</i> , Å	10.6098(6)
<i>b</i> , Å	11.0454(6)
<i>c</i> , Å	15.5814(9)
$\alpha$ , deg	101.428(3)
$\beta$ , deg	97.149(3)
$\gamma$ , deg	94.792(3)
<i>V</i> , Å <sup>3</sup>	1764.84(17)
space group	$P\bar{1}$
<i>Z</i>	2
<i>D<sub>c</sub></i> g/cm <sup>3</sup>	1.469
<i>F</i> (000)	808
$\mu$ , mm <sup>−1</sup>	0.682
radiation	Mo K $\alpha$ , $\lambda = 0.71073$ Å
temperature, K	100(2)
final <i>R</i> indices [ <i>I</i> > 2 $\sigma$ ( <i>I</i> )]	<i>R</i> <sub>1</sub> = 0.0832, <i>wR</i> <sub>2</sub> = 0.2166
final <i>R</i> indices (all data)	<i>R</i> <sub>1</sub> = 0.1037, <i>wR</i> <sub>2</sub> = 0.2408

## RESULTS

The synthesis and spectroscopic characterization for three five-coordinate nitrosyl porphyrinates have been successfully carried out. The porphyrinate species are all related to protoporphyrin IX or heme *b*. Protoporphyrin IX has two vinyl groups at the 3 and 7 positions of the porphine nucleus. These are often noted, trivially, as the 2, 4 positions. The two vinyl groups are reduced to ethyl groups in the mesoporphyrin IX species and converted to hydrogen atoms in the deuteroporphyrin derivative. The other six peripheral substituents remain unchanged (3,8,12,18-tetramethyl and 13,17-dipropionate, cf. Scheme 1). The two acidic propionate side chains are often esterified for synthetic convenience. Methyl esters have been used in the studies reported here. The UV–vis, IR, and EPR data are summarized in Table 2.

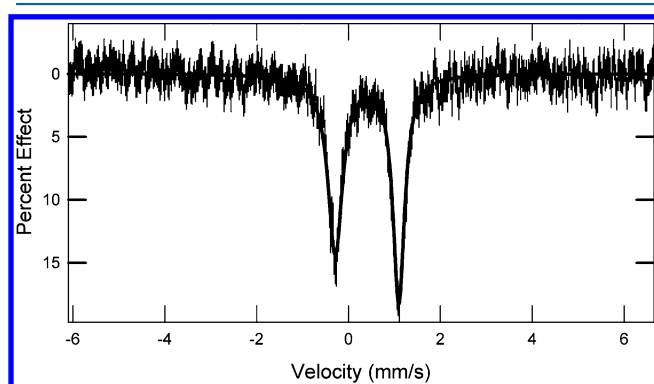
The three nitrosyl complexes have been characterized by Mössbauer spectroscopy in zero and applied magnetic field; all samples were found to be consistent with the presence of a single species. The spectra of all three are sharp, slightly

**Table 2.** UV-vis, IR, and EPR Data for [Fe(PPIX-DME)(NO)], [Fe(DPIX-DME)(NO)], [Fe(MPIX-DME)(NO)], and Related Complexes

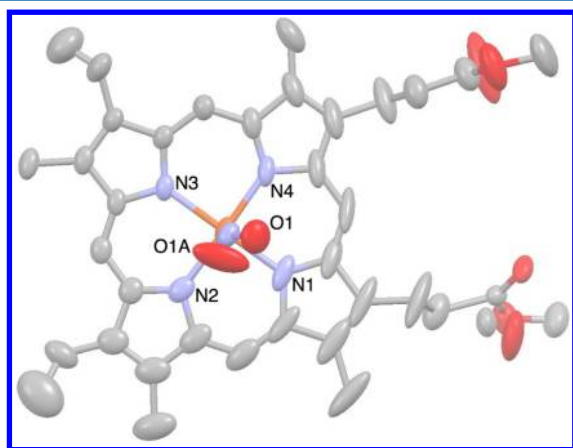
complex	UV-vis, nm	$\nu(\text{NO})$ , $\text{cm}^{-1}$	$\nu(\text{CO})$ , $\text{cm}^{-1}$	$g_1$	$g_2$	$g_3$	$A$ (G)	ref
[Fe(PPIX-DME)(NO)]	395, 480, 543, 568 <sup>a</sup>	1660 <sup>b</sup>	1740 <sup>b</sup>	2.10 <sup>c</sup>	2.06 <sup>c</sup>	2.00 <sup>c</sup>	17 <sup>c</sup>	this work
[Fe(DPIX-DME)(NO)]	388, 473, 530, 555 <sup>a</sup>	1651 <sup>b</sup>	1735 <sup>b</sup>	2.11 <sup>c</sup>	2.06 <sup>c</sup>	2.01 <sup>c</sup>	16 <sup>c</sup>	this work
[Fe(MPIX-DME)(NO)]	390, 478, 525, 560 <sup>a</sup>	1658 <sup>b</sup>	1738 <sup>b</sup>	2.10 <sup>c</sup>	2.06 <sup>c</sup>	2.01 <sup>c</sup>	16 <sup>c</sup>	this work
[Fe(OEP)(NO)]	389, 479, 529, 554 <sup>d,e</sup>	1673 <sup>b,e</sup>	NA	2.11 <sup>f</sup>	2.04 <sup>f</sup>	2.01 <sup>f</sup>	18 <sup>f</sup>	21, 28
[Fe(TPP)(NO)]	405, 537, 606 <sup>a,g</sup>	1700 <sup>h,i</sup> , 1670 <sup>b,g</sup>	NA	2.103 <sup>i</sup>	2.06 <sup>i</sup>	2.01 <sup>i</sup>	17 <sup>i</sup>	17, 29

<sup>a</sup>CHCl<sub>3</sub> solution. <sup>b</sup>KBr pellet. <sup>c</sup>Frozen CH<sub>2</sub>Cl<sub>2</sub> glass at 77 K. <sup>d</sup>CH<sub>2</sub>Cl<sub>2</sub> solution. <sup>e</sup>Data taken from ref 21. <sup>f</sup>Data measured on doped single crystal, ref 28. <sup>g</sup>Data from ref 17. <sup>h</sup>Nujol mull. <sup>i</sup>Data from ref 29.

asymmetric, quadrupole doublets; the zero field spectrum of [Fe(PPIX-DME)(NO)] is shown in Figure 1.

**Figure 1.** The zero field Mössbauer spectrum of [Fe(PPIX-DME)(NO)] at 4.2 K.

The molecular structure of [Fe(PPIX-DME)(NO)] has been determined at 100 K. As noted in the experimental section, there are some modest disorder issues, but the major features of the molecule are clear. A thermal ellipsoid plot of the [Fe(PPIX-DME)(NO)] molecule is given in Figure 2, and a fully labeled diagram with all atom names is given in Figure S1, Supporting Information.

**Figure 2.** Thermal ellipsoid plot of the [Fe(PPIX-DME)(NO)] molecule. Ellipsoids are plotted at the 50% probability level. Hydrogen atoms have been omitted for clarity. The porphyrin ring appears to be pivoting around a point between N2 and N3, that leads to the extended ellipsoids in only a part of the ring.

## DISCUSSION

A major issue for these nitrosyl derivatives of the naturally occurring porphyrins is whether they have significantly different properties from those based on synthetic porphyrins. The N–O stretching frequency of the three are seen to be significantly lower than those of the synthetic species (Table 2). Since Maxwell and Caughey<sup>30</sup> and especially Yoshimura<sup>31</sup> had shown that the N–O stretching frequency in [Fe(PPIX-DME)(NO)] was sensitive to environment, we compare values for all species measured in as close as possible the same conditions. Values for the three new porphyrin species are seen to be lower than those for either the TPP or OEP derivatives. Given the  $\nu(\text{NO})$  sensitivity to environment shown by [Fe(PPIX-DME)(NO)], we thought that these lower NO stretching frequencies might be reflected in interactions between the NO and the polar propionate side chains. A careful examination of the crystalline packing environments of [Fe(PPIX-DME)(NO)] (reported here) and [Fe(MPIX-DME)(NO)]<sup>23</sup> show no such interactions. We conclude that the peripheral groups of the naturally occurring porphyrins have a real effect on the NO stretching frequency.

Gas phase spectra of the NO complex of protoporphyrin IX itself, although protonated on one vinyl group, shows  $\nu(\text{NO})$  of 1720  $\text{cm}^{-1}$ .<sup>32</sup> The  $\nu(\text{NO})$  of the iron(III) species also shows a higher value of than those reported in KBr pellet or in solution.<sup>33</sup>

Although the data are limited, an effect stemming from the peripheral group substituents on the Mössbauer parameters is also observed. Values of the Mössbauer parameters for all three derivatives are given in Table 3. There are only limited Mössbauer data available for other nitrosyls and one previous study in applied magnetic field; these data are also given in Table 3. The Mössbauer parameters for the nitrosyl derivatives show slightly greater quadrupole splitting and isomer shift values in the natural porphyrins compared to TTP and OEP. The increased isomer shift results from greater population of the valence orbitals which, through the resulting screening of the nuclear charge, causes a reduced s-electron density at the nucleus. An increased valence electron population must occur among orbitals that make a positive contribution to the electric field gradient:  $d_{xy}$ ,  $d_{x^2-y^2}$ ,  $p_x$ ,  $p_y$ , in order to result in a corresponding increase in the (positive) quadrupole splitting. This is probably the result of the asymmetric peripheral substitution pattern. The spectroscopic data are thus consistent with a modest difference in the electronic structures of the natural heme derivatives relative to those of the synthetic hemes.

Lang and Marshall<sup>37,38</sup> reported Mössbauer spectra for a number of liganded hemoglobin derivatives including a nitrosyl derivative; their observed NO spectrum showed a broad

Table 3. Mössbauer Data for [Fe(Porph)(NO)] Complexes

complex	$\Delta E_q^{a,b}$	$\delta^a$	$\eta^c$	$A_{xx}/g\mu_B^d$	$A_{yy}/g\mu_B^d$	$A_{zz}/g\mu_B^d$	ref
[Fe(PPIX-DME)(NO)] <sup>e</sup>	+1.39	0.40	0.15	−5.3	−15.7	10.5	this work
[Fe(PPIX-DME)(NO)] <sup>f</sup>	+1.38	0.37					34
[Fe(MPIX-DME)(NO)] <sup>e</sup>	+1.43	0.39	0.23	−3.0	−14.2	10.0	this work
[Fe(DPIX-DME)(NO)] <sup>e</sup>	+1.48	0.38	0.22	−8.8	−16.4	11.0	this work
[Fe(TPP)(NO)] <sup>e</sup>	+1.24	0.35	0.32	−25	−10	13.2	35
[Fe(TPP)(NO)] <sup>e</sup>	1.24	0.35					this work
[Fe(OEP)(NO)] <sup>e</sup>	1.27	0.37					this work
[Fe(OEP)(NO)] <sup>f</sup>	1.26	0.35					36
[Fe(OEP)(NO)] <sup>f</sup>	1.22	0.37					34

<sup>a</sup>Value in mm/s. <sup>b</sup>+ sign determined experimentally. <sup>c</sup>Asymmetry parameter. <sup>d</sup>Value in T. <sup>e</sup>Measured at 4.2 K. <sup>f</sup>Measured at 100 K.

Table 4. Structural Parameters for [Fe(Porph)(NO)] Complexes

complex	Fe–N–O <sup>a</sup>	<Fe–N <sub>p</sub> > <sup>b</sup>	$\Delta Fe(Ct)^{b,c}$	$\Delta Fe(N_4)^{b,d}$	Fe–N <sup>b</sup>	N–O <sup>b</sup>	orientation <sup>a,e</sup>	tilt <sup>a,f</sup>	ref
[Fe(PPIX-DME)(NO)]	143.4(6) <sup>g</sup>	1.998(9)	0.29	0.26	1.719(4)	1.140(8) <sup>g</sup>	36 <sup>g</sup>		this work
[Fe(DPIX-DME)(NO)]	143.1(3)	2.005(21)	0.26	0.26	1.723(3)	1.187(4)	35.0	6.2	23
[Fe(OEP)(NO)] (A)	144.4(2)	2.004(15)	0.29	0.28	1.722(2)	1.167(3)	37.9	6.5	21
[Fe(OEP)(NO)] (B)	142.74(8)	2.010(12)	0.27	0.28	1.7307(7)	1.1677(11)	40.2	8.2	21
[Fe(TPP)(NO)] <sup>h</sup>	144.4(5)	1.999(4)	0.20	0.20	1.739(6)	1.163(5)	44.3	6.3	39
[Fe(TPPBr <sub>4</sub> )(NO)] (A')	147.9(8)	2.01(3)	0.37	0.31	1.734(8)	1.119(11)	0.0	5.6	21
[Fe(TPPBr <sub>4</sub> )(NO)] (A'')	146.9(9)	2.00(2)	0.32	0.30	1.726(9)	1.144(12)	0.0	7.1	21
[Fe(TPPBr <sub>4</sub> )(NO)] (B)	145(1)	1.95(3)	0.29	0.28	1.691(11)	1.145(16)	18.4		21
[Fe(oxoOEC)(NO)]	143.11(15)	2.009(9)	0.26	0.26	1.7320(13)	1.1696(19)	40.9	7.1	21
[Fe(3,5-MeBAFP)(NO)] (A)	146.3(4)	1.991(8)	0.35	<i>i</i>	1.713(4)	1.149(5)	~0	<i>i</i>	40
[Fe(3,5-MeBAFP)(NO)] (B)	146.6(5)	1.993(5)	0.37	<i>i</i>	1.714(4)	1.142(5)	~0	<i>i</i>	40
[Fe(OETAP)(NO)]	143.7(4)	1.932(9)	0.31	<i>i</i>	1.721(4)	1.155(5)	39.6	7.6	36

<sup>a</sup>Value in degrees. <sup>b</sup>Value in Å. <sup>c</sup>Iron atom displacement from 24-atom mean plane. <sup>d</sup>Iron atom displacement from four nitrogen atom plane. <sup>e</sup>Minimum dihedral angle between Fe–N–O and N<sub>p</sub>–Fe–N(NO) planes. <sup>f</sup>Deviation from normal to 24-atom mean plane. <sup>g</sup>Major NO oxygen atom. <sup>h</sup>Triclinic form, 33 K. <sup>i</sup>Not reported.

quadrupole doublet, and the investigators did not give values for the isomer shift and quadrupole splitting constant.

The structural parameters of a number of five-coordinate nitrosyl derivatives are provided in Table 4. Previous structure determinations of heme nitrosyls have revealed a number of distinct structural features. The resolution of these subtle features requires high-quality single crystals and the extensive and accurate data provided by modern area detector diffractometers. Prominent among these features are an off-axis tilt of the Fe–NO bond and a correlated asymmetry in the equatorial Fe–N<sub>p</sub> bonds. These features seemed to be accentuated in the structure of [Fe(DPIX-DME)(NO)] relative to the synthetic porphyrins. The crystallization and structure determination of the protoporphyrin derivative was undertaken to see if indeed these differences were as large in that derivative as well. Unfortunately the structure of [Fe(PPIX-DME)(NO)] is disordered, especially in the axial NO ligand that obscures and limits the statistical significance of any comparisons of equatorial asymmetry and off-axis NO tilt.

The structural parameters found for [Fe(PPIX-DME)(NO)] can be compared with those of [Fe(DPIX-DME)(NO)] and other derivatives found in Table 4. Despite the disorder that would obscure the off-axis tilt and equatorial asymmetry, the geometrical parameters of [Fe(PPIX-DME)(NO)] are comparable to all other nitrosyls. This includes most parameters of the FeNO group other than the (unresolvable) off-axis tilt, which clearly must be greater than 2.5° and likely much larger. Interestingly, the orientation of the major FeNO group (Figure 2) is between the pyrrole groups bearing the propionate side chains, the same orientation as that found for [Fe(DPIX-

DME)(NO)] (with a single NO orientation). This orientation of the NO, with its projection onto the porphyrin plane approximately midway between a pair of equatorial Fe–N<sub>p</sub> bonds, is the most common orientation.

The porphyrin core conformation in [Fe(PPIX-DME)(NO)] is shown in the formal diagram of Figure 3 and is seen to be

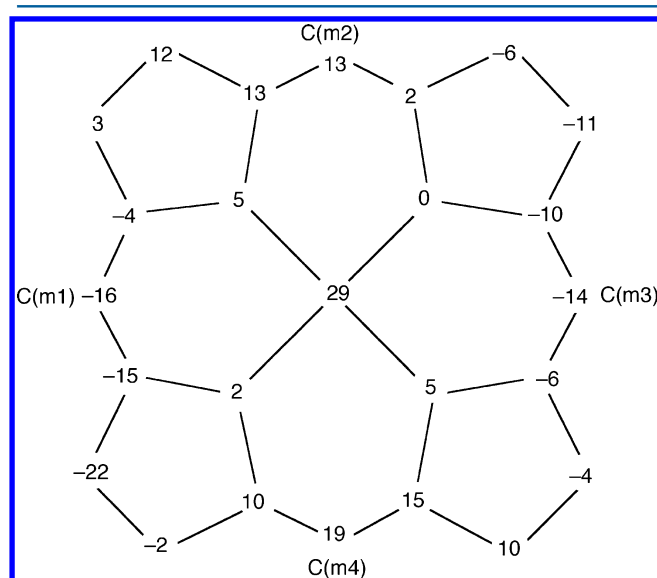
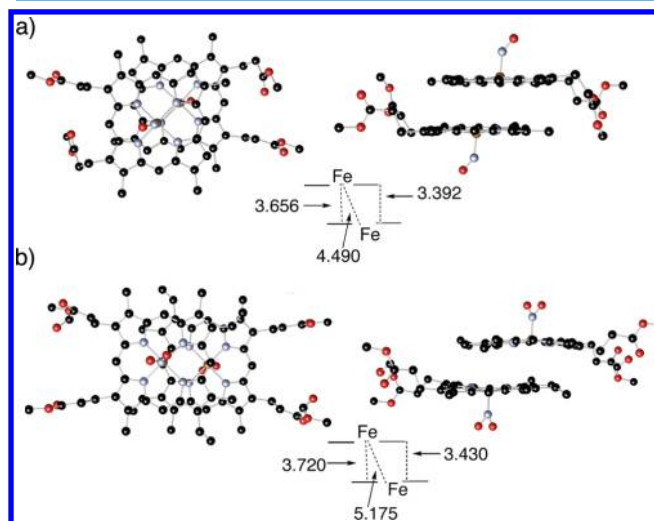


Figure 3. Formal diagram of [Fe(PPIX-DME)(NO)] showing the displacements of each atom from the 24-atom mean plane in units of 0.01 Å. Positive values of the displacement are toward the NO ligand.



ruffled. Although the core conformation of the deuteroporphyrin analogue is also ruffled, it is less so. There does not appear to be a consistent pattern of ring conformations in the nitrosyls listed in Table 4.

One interesting solid-state packing feature is the formation of pairwise interacting molecules as shown in Figure 4. This



**Figure 4.** Diagram illustrating the solid-state interactions for (a)  $[\text{Fe}(\text{DPIX-DME})(\text{NO})]$  and (b)  $[\text{Fe}(\text{PPIX-DME})(\text{NO})]$ . Both top-down and side-on views are given.

feature is seen for both the proto- and deuteroporphyrin complexes. The pairs of molecules are related by inversion symmetry, and thus the two porphyrin rings are precisely parallel. Both top-down and side-on views of the two systems are shown along with some metrics of the interactions. The two complexes have somewhat different lateral shifts for the two overlapped rings. The lateral shift for  $[\text{Fe}(\text{PPIX-DME})(\text{NO})]$  is 3.27 Å, which puts it into the Group I class according to the classification scheme of Scheidt and Lee.<sup>41</sup> The ring overlap in the deuteroporphyrin derivative<sup>23</sup> is tighter with a lateral shift of 2.30 Å, putting this complex in the Class S group. The lateral shifts of these pairwise interactions are, however, much larger than those observed in two different crystalline forms of the  $[\text{Fe}(\text{OEP})(\text{NO})]^+$  cation.<sup>42,43</sup> In those two derivatives, the very strong pairwise interaction leads to lateral shifts of the two rings of 1.32 and 1.43 Å. Interestingly, despite the disordered NO group, the porphyrin peripheral groups are completely ordered; there is no interchange of the methyl and vinyl groups.

## SUMMARY

The spectroscopic properties (UV-vis, IR, EPR, and Mössbauer) of the nitrosyliron(II) derivatives of proto-, deuto- and mesoporphyrin dimethyl esters are reported. These are similar to those of synthetic porphyrin derivatives but are consistent with small differences in electronic structure. These are the presumed result of the asymmetric peripheral substituents compared to the synthetic porphyrins. The molecular structure of  $[\text{Fe}(\text{PPIX-DME})(\text{NO})]$  has been determined and compared with that previously reported for the deuteroporphyrin analogue. Unfortunately, the determination of the magnitude of equatorial Fe-N<sub>p</sub> asymmetry and the off-axis tilt could not be made owing to the NO axial ligand disorder.

## ASSOCIATED CONTENT

### Supporting Information

Figure S1 is the thermal ellipsoid diagram giving the complete atom naming scheme. Figures S2–S4 give the experimental and fitted Mössbauer data. Tables S1–S6 give complete crystallographic details, atomic coordinates, bond distances and angles, anisotropic temperature factors, and fixed hydrogen atom positions for  $[\text{Fe}(\text{PPIX-DME})(\text{NO})]$ . A crystallographic information file (CIF) is also available. This material is available free of charge via the Internet at <http://pubs.acs.org>.

## AUTHOR INFORMATION

### Corresponding Author

\*E-mail: [scheidt.1@nd.edu](mailto:scheidt.1@nd.edu).

### Author Contributions

#G.R.A.W. and N.J.S. contributed equally to this work.

### Notes

The authors declare no competing financial interest.

## ACKNOWLEDGMENTS

We thank the National Institutes of Health for support of this research under Grant GM-38401 to W.R.S.

## REFERENCES

- (1) Culotta, E.; Koshland, D. E. *Science* **1992**, 258, 1862.
- (2) Kots, A. Y.; Martin, E.; Sharina, I. G.; Murad, F. In *Handbook of Experimental Pharmacology*; Schmidt, H. H., Hofmann, F., Stasch, J.-P., Eds.; Springer-Verlag: Berlin, 2009; pp 1–14.
- (3) Russwurm, M.; Koesling, D. *EMBO J.* **2004**, 23, 4443.
- (4) Moncada, S.; Palmer, R. M. J.; Higgs, E. A. *Pharmacol. Rev.* **1991**, 43, 109.
- (5) Snyder, S. H. *Science* **1992**, 257, 494.
- (6) Butler, A. R.; Williams, D. L. H. *Chem. Soc. Rev.* **1993**, 233.
- (7) Stamler, J. S.; Singel, D. J.; Loscalzo, J. *Science* **1992**, 258, 1898.
- (8) Hughes, M. N. *Biochim. Biophys. Acta* **1999**, 1411, 263.
- (9) Walker, F. A. *J. Inorg. Biochem.* **2005**, 99, 216.
- (10) Cooper, C. E. *Biochim. Biophys. Acta* **1999**, 1411, 290.
- (11) Drapier, J.-C.; Pellat, C.; Henry, Y. *J. Biol. Chem.* **1991**, 266, 10162.
- (12) Stadler, J.; Bergonia, H. A.; Di Silvio, M.; Sweetland, M. A.; Billiar, T. R.; Simmons, R. L.; Lancaster, J. R. *Arch. Biochem. Biophys.* **1993**, 302, 4.
- (13) Terenzi, F.; Diaz-Guerra, M. J. M.; Casado, M.; Hortelano, S.; Leoni, S.; Bosca, L. *J. Biol. Chem.* **1995**, 270, 6017.
- (14) Abbreviations used in this paper: PPIX-DME, dianion of protoporphyrin IX dimethyl ester; DPIX-DME, dianion of deuteroporphyrin IX dimethyl ester; MPPIX-DME, dianion of mesoporphyrin IX dimethyl ester; Porph, dianion of a generalized porphyrin; OEP, dianion of octaethylporphyrin; TPP, dianion of meso-tetraphenylporphyrin; TPPBr<sub>4</sub>, dianion of 2,3,12,13-tetrabromo-5,10,15,20-tetraphenylporphyrin; oxoOEC, dianion of (oxooctaethylchlorin), 3,3,7,8,12,13,17,18-octaethyl-(3 H)-porphin-2-onato(2-); OETAP, dianion of octaethyltetraazaporphyrin; 3,5-MeBAFP, dianion of 3,5-methyl-bis(aryloxy)-fenceporphyrin; DMF, dimethylformamide.
- (15) Scheidt, W. R.; Ellison, M. K. *Acc. Chem. Res.* **1999**, 32, 350.
- (16) Wyllie, G. R. A.; Scheidt, W. R. *Chem. Rev.* **2002**, 102, 1067.
- (17) Scheidt, W. R.; Frisse, M. E. *J. Am. Chem. Soc.* **1975**, 97, 17.
- (18) Bohle, D. S.; Hung, C.-H. *J. Am. Chem. Soc.* **1995**, 117, 9584.
- (19) Nasri, H.; Haller, K. J.; Wang, Y.; Huynh, B. H.; Scheidt, W. R. *Inorg. Chem.* **1992**, 31, 3459.
- (20) Ellison, M. K.; Scheidt, W. R. *J. Am. Chem. Soc.* **1997**, 119, 7404.
- (21) Scheidt, W. R.; Duval, H. F.; Neal, T. J.; Ellison, M. K. *J. Am. Chem. Soc.* **2000**, 122, 4651.
- (22) Ellison, M. K.; Scheidt, W. R. *Inorg. Chem.* **1998**, 37, 382.
- (23) Wyllie, G. R. A.; Scheidt, W. R. *Inorg. Chem.* **2003**, 42, 4259.

- (24) Leu, B.; Zgierski, M.; Wyllie, G. R. A.; Scheidt, W. R.; Sturhahn, W.; Alp, E. E.; Durbin, S. M.; Sage, J. T. *J. Am. Chem. Soc.* **2004**, *126*, 4211.
- (25) Dodd, R. E.; Robinson, P. L. *Experimental Inorganic Chemistry*; Elsevier: New York, 1957; p 253.
- (26) Adler, A. D.; Longo, F. R.; Kampas, F.; Kim, J. *J. Inorg. Nucl. Chem.* **1970**, *32*, 2443.
- (27) Sheldrick, G. M. *Acta Crystallogr., Sect. A: Found. Crystallogr.* **2008**, *A64*, 112.
- (28) Hayes, R. G.; Ellison, M. K.; Scheidt, W. R. *Inorg. Chem.* **2000**, *39*, 3665.
- (29) Wayland, B. B.; Olson, L. W. *J. Am. Chem. Soc.* **1974**, *96*, 6037.
- (30) Maxwell, J. C.; Caughey, W. S. *Biochemistry* **1976**, *15*, 388.
- (31) Yoshimura, T. *Bull. Chem. Soc. Jpn.* **1978**, *51*, 1237.
- (32) Lanucara, F.; Scuder, D.; Chiavarino, B.; Fornarini, S.; Ma?tre, P.; Crestoni, M. E. *J. Phys. Chem. Lett* **2013**, *4*, 2414.
- (33) Lanucara, F.; Crestoni, M. E.; Scuder, D.; Sinha, R. K.; Ma?tre, P.; Fornarini, S. *Inorg. Chem.* **2011**, *50*, 4445.
- (34) Bonnet, R.; Charalambides, A. A.; Martin, R. A.; Sales, K. D.; Fitzsimmons, B. W. *J. Chem. Soc., Chem. Commun.* **1975**, 884.
- (35) Nasri, H.; Ellison, M. K.; Chen, S.; Huynh, B. H.; Scheidt, W. R. *J. Am. Chem. Soc.* **1997**, *119*, 6274.
- (36) Bohle, D. S.; Debrunner, P.; Fitzgerald, J.; Hansert, B.; Hung, C.-H.; Thompson, A. J. *J. Chem. Soc., Chem. Commun.* **1997**, 91.
- (37) Lang, G.; Marshall, W. *Proc. Phys. Soc.* **1966**, *87*, 3.
- (38) Lang, G.; Marshall, W. *J. Mol. Biol.* **1966**, *18*, 385.
- (39) Silvernail, N. J.; Olmstead, M. M.; Noll, B. C.; Scheidt, W. R. *Inorg. Chem.* **2009**, *48*, 971.
- (40) Goodrich, L. E.; Roy, S.; Alp, E. E.; Zhao, J.; Hu, M. H.; Lehnert, N. *Inorg. Chem.* **2013**, *52*, 7766.
- (41) Scheidt, W. R.; Lee, Y. J. *Struct. Bonding (Berlin)* **1987**, *64*, 1.
- (42) Scheidt, W. R.; Lee, Y. J.; Hatano, K. *J. Am. Chem. Soc.* **1984**, *106*, 3191.
- (43) Ellison, M. K.; Schulz, C. E.; Scheidt, W. R. *Inorg. Chem.* **2000**, *39*, 5102.